

## Hartree-Fock LAPW approach to the electronic properties of periodic systems

S. Massidda,\* M. Posternak, and A. Baldereschi†

*Institut Romand de Recherche Numérique en Physique des Matériaux (IRRMA),  
PHB-Ecublens, CH-1015 Lausanne, Switzerland*

(Received 28 April 1993)

We present a scheme for calculating the (spin-unrestricted) Hartree-Fock (HF) band structure of periodic solids that uses the accurate linearized-augmented-plane-wave basis set. In contrast with linear-combination-of-atomic-orbitals-like schemes, the convergence of the variational HF results can be easily monitored, and the cumbersome evaluation of multicenter integrals is avoided. Potentials and charge densities are evaluated without any shape approximation, and the singularity due to the long-range nature of the Coulomb potential is handled in reciprocal space. All the elements of the Periodic Table can be equally treated, and the relativistic effects for heavy elements are included as in the standard local-density-approximation case. The method is tested on silicon and diamond, where recent HF calculations are available for comparison. The diagonal Coulomb-hole-plus-screened-exchange approximation can also be implemented with little additional computational effort.

### I. INTRODUCTION

The density functional theory (DFT), especially in its local approximation (LDA), is the basis of the very large majority of the electronic structure calculations performed so far in extended systems. However, in spite of the success in explaining several ground state properties of solids, DFT and LDA are known to present severe limitations.<sup>1</sup> Well-known examples of failures of the LDA and of its spin-dependent counterpart (LSD) include the structural properties of weakly bonded systems (e.g., group II dimers and hydrogen-bonded systems), and the incapability to predict the antiferromagnetic ordering and insulating ground state in some transition-metal oxides. The most notable difficulty of DFT-LDA is related to the excitation energies of semiconductors and insulators: although they are not formally interpretable as quasiparticle energies, the DFT Kohn-Sham one-particle eigenvalues are generally used to discuss the excitation spectra of solids. If the overall description of the energy-band dispersion is reasonable, excitation energies obtained in this way are typically too small by 30–50%, compared to the observed gaps.<sup>1</sup> In fact, the calculation of excitation energies requires more complicated schemes.<sup>2–5</sup>

Several attempts have been made in order to improve the LSD-DFT results. We mention in this respect the self-interaction-corrected (SIC) LSD formalism,<sup>6,7</sup> where the spurious self-interaction effects are subtracted from the effective potential. Another way of improving the LDA is the introduction of gradient corrections;<sup>8</sup> in important cases like small clusters of water molecules<sup>9</sup> and group IIA and IIB dimers,<sup>10</sup> the gradient corrections lead to significant improvements. Recently, Anisimov and coworkers<sup>11</sup> proposed model corrections to DFT-LSD band calculations, using an *ad hoc* exchange-correlation potential based on the Hubbard scheme. They have obtained in this way the expected insulating behavior for cuprates

and for a number of transition-metal monoxides.

An approach completely different from DFT is the Hartree-Fock (HF) approximation. This method has been widely applied to atoms and small molecules, but has not yet received comparable attention from solid state physicists. This can be due to the fact that the computationally faster DFT-based methods are usually preferred, and that correlation effects, which are completely neglected in HF, are generally more important in extended solids than in finite systems. Nevertheless, the HF approximation contains several distinctive features which make it attractive for the study of solids: (i) Contrary to LDA and LSD, the HF method does not require the removal of spurious self-interaction terms. Indeed, the self-interaction term appearing in the Hartree contribution is exactly canceled by an opposite exchange term for the occupied states; (ii) HF corresponds to a well-defined approximation in many-body theory and therefore provides a sound starting point for the inclusion of many-body perturbative corrections which are clearly defined. In consequence, it is desirable to develop accurate and efficient schemes for performing HF calculations in periodic solids.

However, it is well known that HF results have to be improved in order to obtain the correct quantitative value of physical parameters such as the band gap and the valence band width of semiconductors. These quantities require a more sophisticated self-energy model,<sup>4,12</sup> and a much larger computational effort. Nevertheless, it is known that an important part of the error made by HF with the complete neglect of correlation terms can be cured by screening the exchange interaction with a simple diagonal dielectric function. The resulting approximation, called diagonal Coulomb hole plus screened exchange (d-COHSEX),<sup>12</sup> has some predictive power in terms of energy gaps and bandwidths (see later), and can be implemented with little additional effort in the HF procedure.

At the present time, only a few HF schemes for extended systems are available.<sup>13–19</sup> They can be essentially divided into two groups: (i) real-space approaches based on localized basis sets, in which the exchange matrix elements are evaluated as direct lattice sums, and (ii) schemes making use of plane waves as basis functions, and in which the exchange matrix elements are evaluated as sums over reciprocal lattice vectors. While the former approaches require time-consuming four-center integrals, the latter demand a careful treatment of summations in the Brillouin zone, because of the singular behavior of the Coulomb interaction. To the first class belong the all-electron self-consistent schemes of Pisani and co-workers,<sup>13</sup> and of André and co-workers,<sup>14</sup> which use basis sets of atomic orbitals represented in terms of Gaussian functions, and the (non-self-consistent) scheme of Svane<sup>15,16</sup> based on the linear muffin-tin-orbital (LMTO) method in the atomic-sphere approximation (ASA). The second class includes the self-consistent pseudopotential calculations of Ohkoshi<sup>17</sup> and Gygi.<sup>18,19</sup>

One of the most accurate band schemes, the self-consistent linearized-augmented-plane-wave (LAPW) method,<sup>20,21</sup> has been widely used within LDA-DFT, but has not yet been adapted to HF calculations. The all-electron LAPW scheme has the following desirable features: (i) it shares with the plane-wave schemes the ease with which the convergence of the variational results can be monitored, in contrast with LCAO-like basis sets; (ii) the basis size does not increase substantially either for heavy elements, as in LCAO, or for light elements, as in plane-wave pseudopotential approaches; (iii) scalar relativistic effects are easily included; (iv) core states can be recalculated at each self-consistency iteration; (v) general potentials and charge densities can be handled without shape approximations. It is therefore highly desirable to set up a LAPW scheme for HF calculations.

In Sec. II we present the basic formalism and describe how the calculations can be done. The results of test applications to diamond and silicon are given in Sec. III, where they are compared to those obtained with other HF schemes. Indeed, these two systems have been extensively used for comparing band structure methods, and can be therefore considered as standard benchmark cases. The application of our scheme to CaCuO<sub>2</sub> has been published elsewhere<sup>22</sup> and will not be further discussed here. Finally, in Sec. IV we draw our conclusions.

## II. METHOD

### A. Representation of the exchange operator

The central idea behind our representation of the exchange operator is based on the result obtained for several systems<sup>15,19</sup> that the one-electron wave functions calculated for a given crystal with the LDA or the Hartree-Fock schemes are similar to each other. This resemblance suggests the following second variational treatment: at each self-consistency iteration of the HF procedure, the LDA exchange-correlation potential  $V_{xc}^{LDA}$  is obtained in the usual way from HF functions, and the corresponding Schrödinger-like equation is solved<sup>23</sup>

$$\hat{H}^{LDA}\psi_{n\mathbf{k}}^{LDA} = \epsilon_{n\mathbf{k}}^{LDA}\psi_{n\mathbf{k}}^{LDA}. \quad (1)$$

These Bloch wave functions are used as the basis functions for a second variational calculation in which the difference  $\hat{V}_e = \hat{\Sigma}_x - V_{xc}^{LDA}$  between the exchange operator and  $V_{xc}^{LDA}$  is taken into account. We have

$$(\hat{H}^{LDA} + \hat{V}_e)\psi_{n\mathbf{k}}^{HF} = \epsilon_{n\mathbf{k}}^{HF}\psi_{n\mathbf{k}}^{HF}, \quad (2)$$

$$\psi_{n\mathbf{k}}^{HF} = \sum_{n'} z_{nn'}^{HF}\psi_{n'\mathbf{k}}^{LDA}. \quad (3)$$

We are then led to the following secular equation:

$$|(\epsilon_{n\mathbf{k}}^{LDA} - E)\delta_{nn'} + \langle n'\mathbf{k}|\hat{V}_e|n\mathbf{k}\rangle| = 0 \quad (4)$$

where  $|n\mathbf{k}\rangle$  are LDA states. As the operator  $\hat{\Sigma}_x$ , and hence  $\hat{V}_e$ , contains the occupied wave functions, the above procedure needs to be iterated. However, since in most cases the HF and LDA wave functions are very similar,<sup>19</sup> the Hamiltonian matrix for the second variation is already close to diagonal, implying that we do not have to incorporate a large number of unoccupied states in the second variation, and that we do not need many iterations to converge. We have

$$\langle n'\mathbf{k}|\hat{V}_e|n\mathbf{k}\rangle = \langle n'\mathbf{k}|\hat{\Sigma}_x|n\mathbf{k}\rangle - \langle n'\mathbf{k}|V_{xc}^{LDA}|n\mathbf{k}\rangle.$$

The matrix elements  $\langle n'\mathbf{k}|V_{xc}|n\mathbf{k}\rangle$  of the local potential  $V_{xc}$  are straightforward to evaluate, using its known interstitial and sphere representations (see later). The matrix elements of the exchange operator can be written

$$\langle n'\mathbf{k}|\hat{\Sigma}_x|n\mathbf{k}\rangle = -e^2 \sum_{m,\mathbf{q}} \int \frac{\psi_{n'\mathbf{k}}^{*LDA}(\mathbf{r}_1)\psi_{m\mathbf{q}}^{HF}(\mathbf{r}_1)\psi_{m\mathbf{q}}^{*HF}(\mathbf{r}_2)\psi_{n\mathbf{k}}^{LDA}(\mathbf{r}_2)}{|\mathbf{r}_1 - \mathbf{r}_2|} d\mathbf{r}_1 d\mathbf{r}_2, \quad (5)$$

where  $m$  runs over all occupied bands (core and valence), and  $\mathbf{q}$  lies in the first Brillouin zone. In the following, we shall drop, unless necessary for clarity, the superscripts LDA and HF. Introducing now in Eq. (5) the “overlap charge densities” defined by

$$\rho_{m\mathbf{q},n\mathbf{k}}(\mathbf{r}) = e\psi_{m\mathbf{q}}^*(\mathbf{r})\psi_{n\mathbf{k}}(\mathbf{r}), \quad (6)$$

the exchange matrix elements can be rewritten in the

following way:

$$\begin{aligned} \langle n'\mathbf{k}|\hat{\Sigma}_x|n\mathbf{k}\rangle &= - \sum_{m,\mathbf{q}} \int \frac{\rho_{m\mathbf{q},n'\mathbf{k}}^*(\mathbf{r}_1)\rho_{m\mathbf{q},n\mathbf{k}}(\mathbf{r}_2)}{|\mathbf{r}_1 - \mathbf{r}_2|} d\mathbf{r}_1 d\mathbf{r}_2 \\ &= - \sum_{m,\mathbf{q}} \int \rho_{m\mathbf{q},n'\mathbf{k}}^*(\mathbf{r}_1)V_{m\mathbf{q},n\mathbf{k}}(\mathbf{r}_1)d\mathbf{r}_1, \end{aligned} \quad (7)$$

where  $V_{m\mathbf{q},n\mathbf{k}}(\mathbf{r})$  is the ‘‘electrostatic potential’’ associated with the overlap charge density  $\rho_{m\mathbf{q},n\mathbf{k}}(\mathbf{r})$

$$V_{m\mathbf{q},n\mathbf{k}}(\mathbf{r}_1) = \int \frac{\rho_{m\mathbf{q},n\mathbf{k}}(\mathbf{r}_2)}{|\mathbf{r}_1 - \mathbf{r}_2|} d\mathbf{r}_2. \quad (8)$$

Before evaluating these expressions, we first decompose  $\hat{\Sigma}_x$  and  $\langle n'\mathbf{k}|\hat{\Sigma}_x|n\mathbf{k}\rangle$  into valence and core contributions, corresponding to  $m$  running over valence and core bands, respectively,

$$\langle n'\mathbf{k}|\hat{\Sigma}_x|n\mathbf{k}\rangle = \langle n'\mathbf{k}|\hat{\Sigma}_x^v|n\mathbf{k}\rangle + \langle n'\mathbf{k}|\hat{\Sigma}_x^c|n\mathbf{k}\rangle. \quad (9)$$

We consider first the valence contribution. The wave functions are expanded in terms of a set of LAPW basis functions  $\phi_{j\mathbf{k}}$

$$\begin{aligned} \psi_{n\mathbf{k}} &= \sum_j z_{nj}(\mathbf{k})\phi_{j\mathbf{k}} \\ &= \begin{cases} \Omega^{-1/2} \sum_j z_{nj}(\mathbf{k}) \exp(i\mathbf{k}_j \cdot \mathbf{r}), & \mathbf{r} \in I; \\ \sum_L [A_L^\alpha(n\mathbf{k})u_l(r_\alpha) + B_L^\alpha(n\mathbf{k})\dot{u}_l(r_\alpha)]Y_L(\hat{r}_\alpha), & |\mathbf{r} - \boldsymbol{\tau}_\alpha| \leq R_\alpha, \end{cases} \end{aligned} \quad (10)$$

with  $A_L^\alpha(n\mathbf{k}) = \sum_j z_{nj}(\mathbf{k})a_L^\alpha(\mathbf{k}_j)$  and  $B_L^\alpha(n\mathbf{k}) = \sum_j z_{nj}(\mathbf{k})b_L^\alpha(\mathbf{k}_j)$ . In these formulas,  $u_l(r_\alpha)$  and  $\dot{u}_l(r_\alpha)$  are the radial solutions of the scalar-relativistic equation inside the muffin-tin (MT) spheres and their derivatives with respect to the energy,  $\Omega$  is the unit cell volume,  $\mathbf{k}_j = \mathbf{k} + \mathbf{G}_j$ ,  $R_\alpha$  and  $\boldsymbol{\tau}_\alpha$  are the MT radius and position

of atom  $\alpha$ ,  $\mathbf{r}_\alpha = \mathbf{r} - \boldsymbol{\tau}_\alpha$ , and  $L = \{l, m\}$  is a collective angular momentum index. The  $a_L^\alpha(\mathbf{k}_j)$  and  $b_L^\alpha(\mathbf{k}_j)$  coefficients are determined by imposing the continuity of each LAPW basis function and of its radial derivative at the muffin-tin boundaries, and their expression can be found in Refs. 20 and 21. In the LAPW representation, we have

$$\rho_{m\mathbf{q},n\mathbf{k}}(\mathbf{r}) = \begin{cases} \sum_j \rho_{m\mathbf{q},n\mathbf{k}}(\mathbf{G}_j) \exp[i(\mathbf{k} - \mathbf{q} + \mathbf{G}_j) \cdot \mathbf{r}], & \mathbf{r} \in I; \\ \sum_L i^l \rho_{m\mathbf{q},n\mathbf{k}}^L(r_\alpha) Y_L(\hat{r}_\alpha), & r_\alpha \in S_\alpha. \end{cases} \quad (11)$$

We note that  $\rho_{m\mathbf{q},n\mathbf{k}}(\mathbf{G}_j)$  are the Fourier components of the periodic part of the product  $\psi_{m\mathbf{q}}^*(\mathbf{r})\psi_{n\mathbf{k}}(\mathbf{r})$ . The corresponding Fourier series has physical meaning only in the interstitial region, as usual. We obtain the potential (8) by using the method introduced by Weinert.<sup>24</sup> The potential in the interstitial region is calculated by replacing the actual overlap charge density inside the spheres with a smoothly varying pseudodensity having the same multipole moments. After the potential has been obtained at the sphere boundaries from the interstitial expansion, its calculation inside the spheres reduces to solving a standard Dirichlet’s problem with the true density. Following these prescriptions, we compute then the Fourier expansion  $\tilde{\rho}_{m\mathbf{q},n\mathbf{k}}(\mathbf{G}_j)$  of the pseudocharge density [see Eqs. (11)–(30) of Ref. 24], and obtain the potential in both regions

$$V_{m\mathbf{q},n\mathbf{k}}(\mathbf{r}) = \begin{cases} 4\pi \sum_j \frac{\tilde{\rho}_{m\mathbf{q},n\mathbf{k}}(\mathbf{G}_j)}{|\mathbf{k} - \mathbf{q} + \mathbf{G}_j|^2} \exp[i(\mathbf{k} - \mathbf{q} + \mathbf{G}_j) \cdot \mathbf{r}], & \mathbf{r} \in I; \\ \sum_L i^l V_{m\mathbf{q},n\mathbf{k}}^L(r_\alpha) Y_L(\hat{r}_\alpha), & r_\alpha \in S_\alpha. \end{cases} \quad (12)$$

Using now Eqs. (7) and (8), together with convolution product properties, we get for the interstitial contribution to the matrix elements

$$\langle n'\mathbf{k}|\hat{\Sigma}_x^v|n\mathbf{k}\rangle_I = -4\pi \sum_{m,\mathbf{q}} \sum_{i,j} \frac{\rho_{m\mathbf{q},n'\mathbf{k}}^*(\mathbf{G}_i) \tilde{\rho}_{m\mathbf{q},n\mathbf{k}}(\mathbf{G}_j)}{|\mathbf{k} - \mathbf{q} + \mathbf{G}_j|^2} U(\mathbf{G}_i - \mathbf{G}_j), \quad (13)$$

where  $U(\mathbf{G}_i - \mathbf{G}_j)$  is the Fourier transform of the step function. Equation (13) is efficiently evaluated numerically using fast Fourier transforms (FFT). We examine now the contributions from the atomic spheres. We have from (10) and (11)

$$\begin{aligned} \rho_{m\mathbf{q},n\mathbf{k}}^L(r_\alpha) &= e \sum_{L_1, L_2} i^{l_2 - l_1 - l} C_{LL_1}^{L_2} [A_{L_1}^{\alpha*}(m\mathbf{q})A_{L_2}^\alpha(n\mathbf{k})u_{l_1}(r_\alpha)u_{l_2}(r_\alpha) + B_{L_1}^{\alpha*}(m\mathbf{q})A_{L_2}^\alpha(n\mathbf{k})\dot{u}_{l_1}(r_\alpha)u_{l_2}(r_\alpha) \\ &\quad + A_{L_1}^{\alpha*}(m\mathbf{q})B_{L_2}^\alpha(n\mathbf{k})u_{l_1}(r_\alpha)\dot{u}_{l_2}(r_\alpha) + B_{L_1}^{\alpha*}(m\mathbf{q})B_{L_2}^\alpha(n\mathbf{k})\dot{u}_{l_1}(r_\alpha)\dot{u}_{l_2}(r_\alpha)], \end{aligned} \quad (14)$$

where the Gaunt coefficients  $C_{LL_1}^{L_2}$  are defined by

$$C_{LL_1}^{L_2} = \int Y_{L_2}^* Y_L Y_{L_1} d\hat{r}.$$

Expression (14) may be rewritten in an abbreviated form

$$\rho_{m\mathbf{q},n\mathbf{k}}^L(r_\alpha) = e \sum_{l_1, l_2} \sum_{\kappa_1, \kappa_2} T_{m\mathbf{q},n\mathbf{k},\alpha}^{\kappa_1 \kappa_2}(l_1 l_2 L) v_{l_1}^{\kappa_1}(r_\alpha) v_{l_2}^{\kappa_2}(r_\alpha), \quad (15)$$

with

$$\begin{aligned} T_{m\mathbf{q},n\mathbf{k},\alpha}^{\kappa_1 \kappa_2}(l_1 l_2 L) &= i^{l_2 - l_1 - l} \sum_{m_1, m_2} C_{L l_1 m_1}^{l_2 m_2} \mathcal{A}_{l_1 m_1}^{\alpha \kappa_1*}(m\mathbf{q}) \mathcal{A}_{l_2 m_2}^{\alpha \kappa_2}(n\mathbf{k}). \end{aligned} \quad (16)$$

Here, the indices  $\kappa_1$  and  $\kappa_2$  take the values 1 and 2, and  $(\mathcal{A}^{\kappa_i}, v^{\kappa_i})$  represent  $(A, u)$  and  $(B, \dot{u})$ , for  $\kappa_i = 1$  and  $\kappa_i = 2$ , respectively. Solving the boundary value problem for the potential inside the spheres gives

$$V_{m\mathbf{q},n\mathbf{k}}^L(r_\alpha) = \int_0^{R_\alpha} dr' r'^2 \mathcal{G}_l^\alpha(r_\alpha, r') \rho_{m\mathbf{q},n\mathbf{k}}^L(r') + V_{m\mathbf{q},n\mathbf{k}}^L(\mathbf{R}_\alpha) \left(\frac{r_\alpha}{R_\alpha}\right)^l, \quad (17)$$

$$\mathcal{G}_l^\alpha(r, r') = \frac{4\pi}{2l+1} \frac{r_{<}^l}{r_{>}^{l+1}} \left[ 1 - \left(\frac{r_{>}}{R_\alpha}\right)^{2l+1} \right], \quad (18)$$

with the Green's function  $\mathcal{G}^\alpha$  given by

$$\langle n'\mathbf{k} | \hat{\Sigma}_x^v | n\mathbf{k} \rangle_S = - \sum_{m,\mathbf{q}} \sum_{\alpha,L} \left\{ e^2 \sum_{\substack{\kappa_1, \kappa_2 \\ \kappa_3, \kappa_4}} \sum_{\substack{l_1, l_2 \\ l_3, l_4}} T_{m\mathbf{q},n'\mathbf{k},\alpha}^{\kappa_1 \kappa_2 *}(l_1 l_2 L) T_{m\mathbf{q},n\mathbf{k},\alpha}^{\kappa_3 \kappa_4}(l_3 l_4 L) \mathcal{I}_R^\alpha(\kappa_1 \kappa_2 \kappa_3 \kappa_4, l_1 l_2 l_3 l_4, l) \right. \\ \left. + \sum_{l_1, l_2} V_{m\mathbf{q},n\mathbf{k}}^L(\mathbf{R}_\alpha) e \sum_{\kappa_1, \kappa_2} T_{m\mathbf{q},n'\mathbf{k},\alpha}^{\kappa_1 \kappa_2 *}(l_1 l_2 L) \mathcal{I}_S^\alpha(\kappa_1 \kappa_2, l_1 l_2, l) \right\}, \quad (19)$$

where

$$V_{m\mathbf{q},n\mathbf{k}}^L(\mathbf{R}_\alpha) = (4\pi)^2 \sum_j \frac{\tilde{\rho}_{m\mathbf{q},n\mathbf{k}}(\mathbf{G}_j)}{|\mathbf{k} - \mathbf{q} + \mathbf{G}_j|^2} \exp[i(\mathbf{k} - \mathbf{q} + \mathbf{G}_j) \cdot \boldsymbol{\tau}_\alpha] Y_L^*(k - q + G_j) j_l(|\mathbf{k} - \mathbf{q} + \mathbf{G}_j| R_\alpha) \quad (20)$$

is the angular momentum decomposition of the interstitial representation, and the two radial integrals are

$$\mathcal{I}_R^\alpha(\kappa_1 \kappa_2 \kappa_3 \kappa_4, l_1 l_2 l_3 l_4, l) = \int_0^{R_\alpha} r^2 dr \int_0^{R_\alpha} r'^2 dr' v_{l_1}^{\kappa_1}(r) v_{l_2}^{\kappa_2}(r) \mathcal{G}_l^\alpha(r, r') v_{l_3}^{\kappa_3}(r') v_{l_4}^{\kappa_4}(r') \quad (21)$$

and

$$\mathcal{I}_S^\alpha(\kappa_1 \kappa_2, l_1 l_2, l) = \int_0^{R_\alpha} r^2 dr \left(\frac{r}{R_\alpha}\right)^l v_{l_1}^{\kappa_1}(r) v_{l_2}^{\kappa_2}(r). \quad (22)$$

These last integrals contain the multipole moments corresponding to the overlap charge densities. In Eq. (19) they are multiplied by the factors  $V_{m\mathbf{q},n\mathbf{k}}^L(\mathbf{R}_\alpha)$ , which include the contribution of *all* the muffin-tin spheres, thus avoiding the calculation of multicenter integrals. Clearly, symmetry allows one to reduce the number of integrals which have to be evaluated.

We now consider the contribution to the exchange ma-

trix elements from the core states. Assuming that there is no core charge spillover in the interstitial region, only contributions arising from the spheres have to be evaluated, and the techniques used by Dagens and Perrot<sup>25</sup> for the APW method may be applied here with minor modifications. As details may be found in Refs. 25 and 26, we give below only the final results, which take into account that the core shells are closed. A core state in the sphere  $\alpha$  may be written as

$$\psi_{n_c L_c}^\alpha = P_{n_c L_c}(r_\alpha) Y_{L_c}(\hat{r}_\alpha). \quad (23)$$

We have then

$$\langle n'\mathbf{k} | \hat{\Sigma}_x^c | n\mathbf{k} \rangle = -e^2 \sum_{n_c, L_c} \int_{S_\alpha} \frac{P_{n_c L_c}(r_1) Y_{L_c}(\hat{r}_1) \psi_{n'\mathbf{k}}^*(\mathbf{r}_1) P_{n_c L_c}(r_2) Y_{L_c}(\hat{r}_2) \psi_{n\mathbf{k}}(\mathbf{r}_2)}{|\mathbf{r}_1 - \mathbf{r}_2|} d\mathbf{r}_1 d\mathbf{r}_2 \\ = -e^2 \sum_{\substack{\kappa_1, \kappa_2 \\ L_1, l}} \sum_{\substack{n_c, L_c \\ L_1, l}} \left[ \frac{(2l_c + 1)(2l + 1)}{4\pi(2l_1 + 1)} \right]^{\frac{1}{2}} C_{l_0 l_c 0}^{l_1 0} \mathcal{A}_{m_1 l_1}^{\alpha \kappa_1 *}(n'\mathbf{k}) \mathcal{A}_{m_1 l_1}^{\alpha \kappa_2}(n\mathbf{k}) \mathcal{I}_C^\alpha(\kappa_1 \kappa_2, n_c l_c l_1, l), \quad (24)$$

where the radial integral is

$$\mathcal{I}_C^\alpha(\kappa_1 \kappa_2, n_c l_c l_1, l) = \int_0^{R_\alpha} r^2 dr \int_0^{R_\alpha} r'^2 dr' P_{n_c L_c}(r) v_{l_1}^{\kappa_1}(r) \mathcal{G}_l(r, r') P_{n_c L_c}(r') v_{l_1}^{\kappa_2}(r'), \quad (25)$$

and the Green's function  $\mathcal{G}$  for these boundary conditions is

$$\mathcal{G}_l(r, r') = \frac{4\pi}{2l+1} \frac{r_{<}^l}{r_{>}^{l+1}}. \quad (26)$$

If we assume that the core wave functions are the same in LDA and in HF, then the expressions given above al-

low us to calculate all necessary matrix elements of the exchange operator, as far as energy bands are concerned. However, a complete HF calculation which includes also the core states can be done without too much extra effort, since the additional core-core and valence-core exchange terms can easily be calculated, by taking advantage of the closed shell structure of the core.

### B. Treatment of the Coulomb singularity

The heaviest part in the computation of the matrix elements (5) is the sum over occupied states, requiring the evaluation of Bloch functions everywhere in the Brillouin zone. Summations over  $\mathbf{q}$  points are usually evaluated using the special-point technique. Such an approach, however, would converge very slowly here, since the long-range nature of the Coulomb interaction produces a singular behavior of the interstitial contribution (13) when  $\mathbf{q} = \mathbf{k} + \mathbf{G}_0$  (where  $\mathbf{G}_0$  is a reciprocal-lattice vector). The same problem shows up in real-space approaches,

$$\bar{\rho}_{m\mathbf{q},n\mathbf{k}}(\mathbf{G}_j) = \int_I \rho_{m\mathbf{q},n\mathbf{k}}(\mathbf{r}) \exp[-i(\mathbf{k} - \mathbf{q} + \mathbf{G}_j) \cdot \mathbf{r}] d\mathbf{r} + \sum_{\alpha} \int_{S_{\alpha}} \rho_{m\mathbf{q},n\mathbf{k}}(\mathbf{r}) \exp[-i(\mathbf{k} - \mathbf{q} + \mathbf{G}_j) \cdot \mathbf{r}] d\mathbf{r}, \quad (28)$$

which clearly shows that both the interstitial region and the atomic spheres contribute to the singularity (27). It has to be noted that the quantity  $\bar{\rho}_{m\mathbf{q},n\mathbf{k}}(\mathbf{G}_j)$  defined above has not the same meaning as  $\rho_{m\mathbf{q},n\mathbf{k}}(\mathbf{G}_j)$  in Sec. II A, where the Fourier components were constructed from the interstitial representation of the wave functions over the whole unit cell. In order to avoid the slow convergence resulting from direct application of the

where it is the sum over neighboring atoms which converges slowly. The analytic properties of the exchange matrix elements have been studied by Gygi,<sup>19</sup> who has shown that expressions such as (13) have for  $\mathbf{q} = \mathbf{k} + \mathbf{G}_0$  an integrable divergence of the form

$$\frac{\bar{\rho}_{m\mathbf{k}+\mathbf{G}_0,n'\mathbf{k}}^*(\mathbf{G}_0)\bar{\rho}_{m\mathbf{k}+\mathbf{G}_0,n\mathbf{k}}(\mathbf{G}_0)}{|\mathbf{k} - \mathbf{q} + \mathbf{G}_0|^2}, \quad (27)$$

where we introduce<sup>27</sup> the Fourier representation of  $\rho_{m\mathbf{q},n\mathbf{k}}(\mathbf{r})$

special-point method, we follow Gygi<sup>18,19</sup> by adding and subtracting to the right-hand side of (13) an auxiliary function  $F(\mathbf{q})$  which has the same singularities as (27). In addition, we note that when both  $\mathbf{k}$  and  $\mathbf{q}$  are inside the first Brillouin zone (as it happens during the self-consistency cycles using the mean-value points), the divergence occurs for  $\mathbf{G}_0 = \mathbf{0}$ . In this particular case, we can write the singular part of the matrix elements as

$$\begin{aligned} \langle n'\mathbf{k} | \hat{\Sigma}_x^v | n\mathbf{k} \rangle_{\text{sing}} = & -4\pi \left\{ \sum_{m,\mathbf{q}} \left[ \frac{\bar{\rho}_{m\mathbf{q},n'\mathbf{k}}^*(\mathbf{0})\bar{\rho}_{m\mathbf{q},n\mathbf{k}}(\mathbf{0})}{|\mathbf{k} - \mathbf{q}|^2} - \bar{\rho}_{m\mathbf{k},n'\mathbf{k}}^*(\mathbf{0})\bar{\rho}_{m\mathbf{k},n\mathbf{k}}(\mathbf{0})F(\mathbf{k} - \mathbf{q}) \right] \right. \\ & \left. + \sum_m \bar{\rho}_{m\mathbf{k},n'\mathbf{k}}^*(\mathbf{0})\bar{\rho}_{m\mathbf{k},n\mathbf{k}}(\mathbf{0}) \sum_{\mathbf{q}} F(\mathbf{k} - \mathbf{q}) \right\}. \end{aligned} \quad (29)$$

In the above equation, we have used the equality  $\bar{\rho}_{m\mathbf{q},n\mathbf{k}}(\mathbf{0}) = \tilde{\rho}_{m\mathbf{q},n\mathbf{k}}(\mathbf{0})$ , which results from the fact that the pseudocharge density preserves the integrated charge within each atomic sphere. The term in square brackets is now regular, and can be evaluated by the special-point technique. The last term on the right-hand side of (29) depends on the choice of the auxiliary function  $F(\mathbf{q})$ . This choice is not critical, except that away from the divergence,  $F(\mathbf{q})$  should be smooth enough. Furthermore, periodicity of  $F(\mathbf{q})$  ensures that its gradient is continuous at the border of the Brillouin zone. We have taken the following choice of the auxiliary function:

$$F(\mathbf{q}) = \frac{1}{\Omega} \sum_j \frac{\exp(-\alpha|\mathbf{q} + \mathbf{G}_j|^2)}{|\mathbf{q} + \mathbf{G}_j|^2}, \quad (30)$$

where  $\alpha$  is a parameter whose value is chosen in order to have a Gaussian width comparable to the Brillouin zone diameter. Its mean value is

$$\frac{\Omega}{(2\pi)^3} \int_{BZ} F(\mathbf{q}) d\mathbf{q} = \frac{1}{(2\pi)^3} 2\alpha \left( \frac{\pi}{\alpha} \right)^{\frac{3}{2}}. \quad (31)$$

### C. GW formalism and related approximations

In the one-particle Green's function formalism, the quasiparticle energies  $\epsilon_{n\mathbf{k}}$  and the corresponding Bloch functions  $\psi_{n\mathbf{k}}(\mathbf{r})$  can be obtained from the solutions of the equation

$$\begin{aligned} \hat{H}\psi_{n\mathbf{k}}(\mathbf{r}) &= \hat{H}_0\psi_{n\mathbf{k}}(\mathbf{r}) + \int d\mathbf{r}' \hat{\Sigma}(\mathbf{r}, \mathbf{r}'; \epsilon_{n\mathbf{k}})\psi_{n\mathbf{k}}(\mathbf{r}') \\ &= \epsilon_{n\mathbf{k}} \psi_{n\mathbf{k}}(\mathbf{r}). \end{aligned} \quad (32)$$

The Hamiltonian  $\hat{H}_0$  includes the kinetic energy operator, the electrostatic potential of the ions, and the Hartree term due to the electrons, while the self-energy operator  $\hat{\Sigma}$  describes the effects of exchange and correlation. A systematic way of constructing approximations of the self-energy operator has been proposed by Hedin.<sup>12</sup> The simplest approximation within this scheme is the so-called GW approximation,<sup>12</sup> where the self-energy is expanded in the *screened* Coulomb interaction, retaining only the lowest term

$$\hat{\Sigma}^{\text{GW}}(\mathbf{r}, \mathbf{r}'; E) = i \int \frac{dE'}{2\pi} G(\mathbf{r}, \mathbf{r}'; E + E') \hat{W}(\mathbf{r}, \mathbf{r}'; E'). \quad (33)$$

$G$  is the one-particle Green's function, expressed in a quasiparticle approximation as

$$G(\mathbf{r}, \mathbf{r}'; E) = \sum_{m, \mathbf{q}} \frac{\psi_{m\mathbf{q}}(\mathbf{r}) \psi_{m\mathbf{q}}^*(\mathbf{r}')}{E - \epsilon_{m\mathbf{q}} + i\eta \text{sgn}(\epsilon_{m\mathbf{q}} - \mu)}, \quad (34)$$

where  $\mu$  is the Fermi energy, and the sum over  $m$  and  $\mathbf{q}$  runs over *all* (occupied and empty) states in the first Brillouin zone.  $\hat{W}$  is the dynamically screened Coulomb interaction

$$\hat{W}(\mathbf{r}, \mathbf{r}'; E) = \int d\mathbf{r}'' \hat{\epsilon}^{-1}(\mathbf{r}, \mathbf{r}''; E) v(\mathbf{r}'' - \mathbf{r}'), \quad (35)$$

$$\hat{W}(\mathbf{q} + \mathbf{G}_i, \mathbf{q} + \mathbf{G}_j; E) = v(\mathbf{q} + \mathbf{G}_j) \delta_{\mathbf{G}_i, \mathbf{G}_j} + v(\mathbf{q} + \mathbf{G}_j) [\hat{\epsilon}^{-1}(\mathbf{q} + \mathbf{G}_i, \mathbf{q} + \mathbf{G}_j; E) - \delta_{\mathbf{G}_i, \mathbf{G}_j}]. \quad (37)$$

If we substitute this expression for  $\hat{W}$  into (33), the first term (bare Coulomb interaction) gives the HF self-energy, and the second term gives the correlation corrections due to the dynamical screening. We finally get

$$\langle n'\mathbf{k} | \hat{\Sigma}^{\text{GW}} | n\mathbf{k} \rangle = \langle n'\mathbf{k} | \hat{\Sigma}^{\text{HF}} | n\mathbf{k} \rangle - 4\pi \sum_{m, \mathbf{q}} \sum_{i, j} \frac{\bar{\rho}_{m\mathbf{q}, n'\mathbf{k}}^*(\mathbf{G}_i) \bar{\rho}_{m\mathbf{q}, n\mathbf{k}}(\mathbf{G}_j)}{|\mathbf{k} - \mathbf{q} + \mathbf{G}_j|^2} \times \int \frac{[\hat{\epsilon}^{-1}(\mathbf{k} - \mathbf{q} + \mathbf{G}_i, \mathbf{k} - \mathbf{q} + \mathbf{G}_j; E') - \delta_{\mathbf{G}_i, \mathbf{G}_j}] dE'}{E + E' - \epsilon_{m\mathbf{q}} + i\eta \text{sgn}(\epsilon_{m\mathbf{q}} - \mu)} \frac{dE'}{2\pi}, \quad (38)$$

where we have used the Fourier components  $\bar{\rho}_{m\mathbf{q}, n\mathbf{k}}(\mathbf{G}_j)$  defined in Sec. II B. The calculation of the HF contribution  $\langle n'\mathbf{k} | \hat{\Sigma}^{\text{HF}} | n\mathbf{k} \rangle$  has already been discussed in Secs. II A and II B. In order to evaluate the correlation contribution,  $\langle n'\mathbf{k} | \hat{\Sigma}^{\text{GW}} - \hat{\Sigma}^{\text{HF}} | n\mathbf{k} \rangle$ , we first notice that  $\epsilon^{-1} - 1$  vanishes quickly at large wave vectors, resulting in a fast convergence of the expansion in terms of  $\mathbf{G}_i$  and  $\mathbf{G}_j$ . This allows us to perform the double reciprocal-lattice-vector summation in (38), which otherwise would be practically impossible in an all-electron approach. In order to perform this summation, we have to evaluate

$$\int_{S_\alpha} \rho_{m\mathbf{q}, n\mathbf{k}}(\mathbf{r}) \exp[-i\mathbf{K}_j \cdot \mathbf{r}] d\mathbf{r} = 4\pi e \exp[-i\mathbf{K}_j \cdot \boldsymbol{\tau}_\alpha] \sum_L Y_L(\hat{K}_j) \sum_{l_1, l_2} \sum_{\kappa_1, \kappa_2} T_{m\mathbf{q}, n\mathbf{k}, \alpha}^{\kappa_1, \kappa_2}(l_1 l_2 L) \times \int_0^{R_\alpha} r^2 dr j_l(K_j r) v_{l_1}^{\kappa_1}(r) v_{l_2}^{\kappa_2}(r), \quad (40)$$

where use has been made of Eqs. (11) and (15).

The energy integration in Eq. (38) is a non-trivial task, requiring the full dielectric matrix  $\hat{\epsilon}^{-1}(\mathbf{q} + \mathbf{G}_i, \mathbf{q} + \mathbf{G}_j; E)$ , which in turn has to be determined self-consistently. At this point, various approximations can be obtained, depending on the model used to evaluate the energy integral.

The static COHSEX approximation of Hedin<sup>12</sup> consists in assuming a simple plasmon-pole behavior for

where  $v$  is the bare Coulomb interaction and  $\hat{\epsilon}^{-1}$  the dielectric matrix.

The LAPW scheme can also be used efficiently for self-energy calculations within the GW approximation. It is again convenient to use the second variation introduced in Sec. II A, and construct the LDA functions which diagonalize the LDA-like Hamiltonian obtained from quasiparticle functions. In order to calculate the matrix elements of the self-energy operator (33) over the LDA basis, we first Fourier transform Eq. (35)

$$\begin{aligned} \hat{W}(\mathbf{q} + \mathbf{G}_i, \mathbf{q} + \mathbf{G}_j; E) \\ = v(\mathbf{q} + \mathbf{G}_j) \hat{\epsilon}^{-1}(\mathbf{q} + \mathbf{G}_i, \mathbf{q} + \mathbf{G}_j; E), \end{aligned} \quad (36)$$

and then rewrite it as

the Fourier coefficients (28) taking into account both the interstitial and the sphere contributions. The former is efficiently computed with FFT. In order to evaluate the latter, we write  $\mathbf{K}_j = \mathbf{k} - \mathbf{q} + \mathbf{G}_j$  for convenience, and use the Rayleigh expansion of a plane wave

$$\begin{aligned} \exp[-i\mathbf{K}_j \cdot \mathbf{r}] &= 4\pi \exp[-i\mathbf{K}_j \cdot \boldsymbol{\tau}_\alpha] \\ &\times \sum_L i^{-L} Y_L^*(\hat{r}_\alpha) Y_L(\hat{K}_j) j_L(K_j r_\alpha). \end{aligned} \quad (39)$$

We have then

the dynamical dielectric matrix, and taking the limit  $E - \epsilon_{m\mathbf{q}} \ll \hbar\omega_p$ , where  $\omega_p$  is the plasmon frequency. With this approximation, the self-energy breaks into two terms, i.e., Coulomb hole (COH) and screened exchange (SEX)

$$\hat{\Sigma}^{\text{COHSEX}} = \hat{\Sigma}^{\text{COH}} + \hat{\Sigma}^{\text{SEX}}, \quad (41)$$

whose matrix elements can be written explicitly as follows:

$$\begin{aligned} \langle n' \mathbf{k} | \hat{\Sigma}^{\text{SEX}} | n \mathbf{k} \rangle &= \langle n' \mathbf{k} | \hat{\Sigma}^{\text{HF}} | n \mathbf{k} \rangle - 4\pi \sum_{i,j,\mathbf{q}} [\hat{\epsilon}^{-1}(\mathbf{k} - \mathbf{q} + \mathbf{G}_i, \mathbf{k} - \mathbf{q} + \mathbf{G}_j; E = 0) - \delta_{\mathbf{G}_i, \mathbf{G}_j}] \\ &\quad \times \sum_m^{\text{occ}} \frac{\bar{\rho}_{m\mathbf{q},n'\mathbf{k}}^*(\mathbf{G}_i) \bar{\rho}_{m\mathbf{q},n\mathbf{k}}(\mathbf{G}_j)}{|\mathbf{k} - \mathbf{q} + \mathbf{G}_j|^2}, \end{aligned} \quad (42)$$

and

$$\langle n' \mathbf{k} | \hat{\Sigma}^{\text{COH}} | n \mathbf{k} \rangle = 4\pi \sum_{i,j,\mathbf{q}} [\hat{\epsilon}^{-1}(\mathbf{k} - \mathbf{q} + \mathbf{G}_i, \mathbf{k} - \mathbf{q} + \mathbf{G}_j; E = 0) - 1] \sum_m \frac{\bar{\rho}_{m\mathbf{q},n'\mathbf{k}}^*(\mathbf{G}_i) \bar{\rho}_{m\mathbf{q},n\mathbf{k}}(\mathbf{G}_j)}{2|\mathbf{k} - \mathbf{q} + \mathbf{G}_j|^2}. \quad (43)$$

The sum over  $m$  in (42) is over occupied bands only, while that in (43) is over all bands, i.e., over a complete set, thus allowing us to simplify the Coulomb-hole term to a local interaction

$$\langle n' \mathbf{k} | \hat{\Sigma}^{\text{COH}} | n \mathbf{k} \rangle = 4\pi e \sum_{i,j} \bar{\rho}_{n'\mathbf{k},n\mathbf{k}}(\mathbf{G}_j - \mathbf{G}_i) \sum_{\mathbf{q}} \frac{\hat{\epsilon}^{-1}(\mathbf{k} - \mathbf{q} + \mathbf{G}_i, \mathbf{k} - \mathbf{q} + \mathbf{G}_j; E = 0) - 1}{2|\mathbf{k} - \mathbf{q} + \mathbf{G}_j|^2}. \quad (44)$$

The bare Coulomb potential appearing in (13) is replaced in Eq. (42) and Eq. (44) by a screened potential, and accordingly, the auxiliary function  $F(\mathbf{q})$  should also be scaled by  $\epsilon(\mathbf{q} = 0)$ .

These formulas can be further simplified by introducing the so-called d-COHSEX approximation. It consists in neglecting local-field effects in the static dielectric screening, which is equivalent to the assumption that the dielectric response of the system has full translational invariance. In this case, the dielectric matrix is diagonal in reciprocal space, and can be replaced by a dielectric function. Equation (36) becomes a simple product

$$\hat{W}(\mathbf{q} + \mathbf{G}_i, \mathbf{q} + \mathbf{G}_j; E) = v(\mathbf{q} + \mathbf{G}_i) \epsilon^{-1}(\mathbf{q} + \mathbf{G}_i) \delta_{\mathbf{G}_i, \mathbf{G}_j}. \quad (45)$$

It is easy to show<sup>28</sup> that the Coulomb-hole contribution Eq. (44) reduces to a constant

$$\langle n' \mathbf{k} | \hat{\Sigma}^{\text{d-COH}} | n \mathbf{k} \rangle = e^2 \delta_{n',n} \frac{1}{(2\pi)^2} \int_{BZ} \frac{\epsilon^{-1}(\mathbf{q}) - 1}{|\mathbf{q}|^2} d\mathbf{q}, \quad (46)$$

while the screened exchange term of Eq. (42) becomes

$$\langle n' \mathbf{k} | \hat{\Sigma}^{\text{d-SEX}} | n \mathbf{k} \rangle = \langle n' \mathbf{k} | \hat{\Sigma}_x | n \mathbf{k} \rangle - 4\pi \sum_{j,\mathbf{q}} [\epsilon^{-1}(\mathbf{k} - \mathbf{q} + \mathbf{G}_j) - 1] \sum_m^{\text{occ}} \frac{\bar{\rho}_{m\mathbf{q},n'\mathbf{k}}^*(\mathbf{G}_j) \bar{\rho}_{m\mathbf{q},n\mathbf{k}}(\mathbf{G}_j)}{|\mathbf{k} - \mathbf{q} + \mathbf{G}_j|^2}. \quad (47)$$

This last formula has been used for testing our formalism, and the results are presented in the next section.

### III. RESULTS

#### A. Computational details

We have tested the above HF-LAPW approach with electronic calculations for silicon and diamond. In order to compare the results of our scheme with those from other existing HF calculations, we used the observed values of the lattice constant 5.430 Å and 3.567 Å (Ref. 29) for silicon and diamond, respectively. The atomic sphere radii are 2.1 (1.4) a.u., and the LAPW basis size has been set to include all plane waves with energy up to 6.3 (14.4) Ry. Similarly, charge densities and potentials have been expanded up to a cutoff of 41 (94) Ry. The wave functions are expanded inside the spheres in terms of products of radial functions and spherical harmonics with  $l \leq 8$ . Charge densities and potentials are expanded up to  $l \leq 8$ . The summations over the Brillouin zone are evaluated using the special-point technique. For both silicon and diamond, we use the two Chadi-Cohen<sup>32</sup> points

$\mathbf{k}_1 = (\frac{3}{4}, \frac{1}{4}, \frac{1}{4})$  and  $\mathbf{k}_2 = (\frac{1}{4}, \frac{1}{4}, \frac{1}{4})$  (in units of  $2\pi/a$ , where  $a$  is the lattice constant), whose stars contain 24 and 8 symmetry-equivalent points, respectively.

The  $\mathbf{q}$  summation over the Brillouin zone in Eq. (5), and the evaluation of the matrix elements of the exchange operator over the LAPW basis, are features of our HF scheme. The  $\mathbf{k}_1, \mathbf{k}_2$  Chadi-Cohen special points are also used for the  $\mathbf{q}$  summation in Eq. (5). However, the time-consuming matrix elements in Eq. (5) do not need to be evaluated 32 times (i.e., over the whole stars of  $\mathbf{k}_1$  and  $\mathbf{k}_2$ ), since symmetry arguments can be used. Indeed, given the point-group symmetry of the exchange operator  $\hat{\Sigma}_x$ , it is easily shown that all matrix elements with  $\mathbf{k} - \mathbf{q}$  belonging to the same star are equal to each other. This fact allows us to restrict, for a given  $\mathbf{k}$ , the number of Bloch functions  $\psi_{m\mathbf{q}}(\mathbf{r})$  which have to be calculated during the self-consistency cycles. Also, once the HF wave functions at a given  $\mathbf{k}$  point have been calculated, those at equivalent points can be obtained by using group-theory methods. Even using symmetry arguments at best, the computation of the exchange contribution to the Hamiltonian matrix elements is rather time-consuming and, in order to save further time in the evaluation of matrix elements (19), summations over  $l, l_1, l_2, l_3, l_4$  are

performed only up to values  $\leq 4$ . This truncation results in an error smaller than 1 mRy on the calculated eigenvalues. LDA-LAPW wave functions are used to start the self-consistency HF process; they are obtained with the same values of convergence parameters. We stress again here that in a HF calculation, the quantities which must be calculated iteratively are the wave functions of the occupied states, and not the total charge density, as for a LDA calculation. However, the closeness of the LDA and HF wave functions in the case of silicon and diamond reduces largely the number of HF iterations, as already pointed out by several authors.<sup>16,19,33</sup> After four iterations, we obtained very good self-consistency for the two crystals studied here, but already the first iteration based on LDA wave functions gives results which are quite close to the final ones. The situation was different for  $\text{CaCuO}_2$ , where 10–15 iterations were needed.

An additional comment is in order regarding the computation of the HF energy band structure, once the self-consistency cycle is over. The computation of the singular terms (29) requires the knowledge of the overlaps  $\tilde{\rho}_{m\mathbf{k},n\mathbf{k}}(\mathbf{0})$  between HF and basis functions at  $\mathbf{k}$ . During the self-consistency procedure, these quantities are calculated only at special points. However, when we calculate the HF band structure at a point  $\mathbf{k}$  which does not belong to the special point set, we need the overlaps between the HF wave functions and basis functions at  $\mathbf{k}$ , which are not known. Therefore, in this case we need to implement a small iteration procedure, in which such overlaps are calculated. Practically, we assume  $\tilde{\rho}_{m\mathbf{k},n\mathbf{k}} = e\delta_{m,n}$ , calculate the first approximation of  $\psi_{n\mathbf{k}}$ , use them to compute the overlaps, and iterate (typically 10–15 times) until the procedure converges. In cases where  $\mathbf{k}$  is close to one of the mean-value points, the denominator of the singular terms becomes very small, and some care is needed for the above procedure to converge. One possible method for avoiding this difficulty is to mix the current overlaps with previous ones during the iterations. Since we only have to iterate on the singular terms, the time-consuming matrix elements do not need to be recalculated, and the required extra time is very small.

### B. Results for silicon and diamond

The HF band structures of silicon and diamond obtained with our formalism are displayed in Figs. 1 and 2. The (self-consistent) energies of the most relevant states relative to the valence band maximum are summarized in Tables I and II, where comparison is made with two recent calculations.<sup>18,19,15</sup> We also list in these tables the corresponding LDA and experimental results. We have not included here data from the pioneer work on silicon by Dovesi, Causà, and Angonoa<sup>34</sup> because of the lack of convergence of their conduction states. We note that the agreement between the LAPW and the pseudopotential calculations is good for both LDA and HF results. The somewhat larger differences relative to the LMTO results may be attributed to the fact that this last calculation (which is not self-consistent) uses the so-called atomic-sphere approximation. In Fig. 3, we compare the

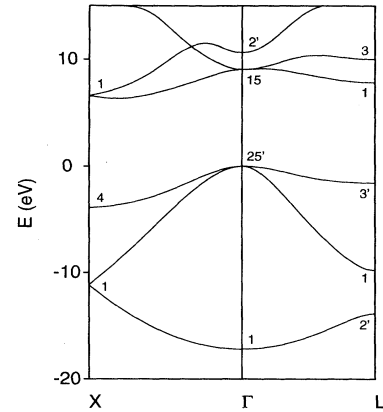


FIG. 1. Hartree-Fock self-consistent band structure of silicon. Energies are measured relative to the valence-band maximum.

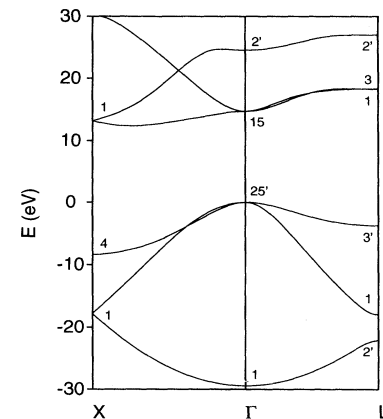


FIG. 2. Hartree-Fock self-consistent band structure of diamond. Energies are measured relative to the valence-band maximum.

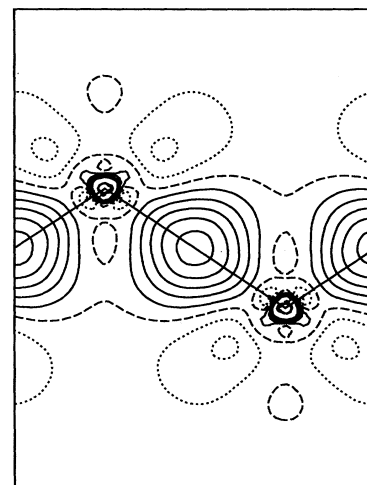


FIG. 3. Difference between the self-consistent Hartree-Fock and LDA charge densities of silicon in the (110) plane. The lines of equal densities are separated by  $0.001 e/(\text{a.u.})^3$ . Broken lines indicate the zero contours, while positive (negative) contours are represented by solid (dotted) lines.

TABLE I. Self-consistent Hartree-Fock eigenvalues and gap  $E_g$  for silicon, as obtained in this work (LAPW) and in other calculations. LDA and experimental values are also given for comparison. Energies are measured in eV with respect to the valence-band maximum.

	LDA (eV)			HF (eV)			Expt. (eV)
	PP <sup>a</sup>	LMTO <sup>b</sup>	LAPW	PP <sup>a</sup>	LMTO <sup>b</sup>	LAPW	
$\Gamma_{1v}$	-12.1	-12.0	-12.0	-17.1	-18.0	-17.1	-12.5 <sup>c</sup>
$\Gamma_{15c}$	2.6	2.7	2.6	9.3	8.7	9.0	3.4 <sup>c</sup>
$\Gamma_{2'c}$	3.4	3.0	3.1	11.0	9.3	10.6	4.2 <sup>c</sup>
$X_{1c}$	0.6		0.6	6.9	5.6	6.6	1.3 <sup>d</sup>
$L_{1c}$	1.5		1.4	8.1	6.7	7.8	2.1 <sup>e</sup> 2.4 <sup>d</sup>
$E_g$	0.5	0.5	0.5	6.4	5.6	6.3	1.2 <sup>c</sup>
$X_{4v} \rightarrow X_{1c}$	3.5		3.5	10.7	10.0	10.5	4.2 <sup>d</sup> 4.5 <sup>c</sup>
$L_{3'v} \rightarrow L_{1c}$	2.7		2.6	9.6	8.1	9.4	3.5 <sup>c</sup> 3.9 <sup>d</sup>

<sup>a</sup>Pseudopotential calculation, Ref. 18.

<sup>b</sup>LMTO calculation, Ref. 15.

<sup>c</sup>From Ref. 29.

<sup>d</sup>From Ref. 30.

<sup>e</sup>From Ref. 31.

total charge densities obtained with the HF and the LDA methods for silicon. The results show that the electronic density is slightly higher in the bond region when the HF approximation is used. This variation only involves a change of about 6% at the bond site, which confirms the resemblance between HF and LDA states.

As usual, HF gaps are larger than the experimental values by a factor of 2 or more, and the valence bandwidths are also larger by about 30–40%. However, HF results can be used as a well-defined starting point for the inclusion of many-body corrections. In particular, HF is a necessary step towards a full GW calculation,<sup>4</sup> which unfortunately requires sophisticated additional calculations (such as, e.g., the full dielectric matrix). However, with little additional computational effort, we can implement the COHSEX method, especially in its diagonal approximation. Although it is known that the d-COHSEX approximation is too crude for correctly predicting the ex-

citation spectrum of semiconductors, it is interesting to compare it with the HF approximation, and to see that much of the quantitative error is removed. We have applied the formalism described in Sec. II C and performed non-self-consistent d-COHSEX calculations in silicon and diamond. We use the following model diagonal dielectric function:

$$\epsilon(q) = \frac{q^2 + \alpha^2}{q^2 + \alpha^2/\epsilon_0} \quad (48)$$

for screening the interaction potential appearing in (47).

We take for silicon (diamond) the experimental values  $\epsilon_0=11.4$  (5.7) and the values  $\alpha=0.93$  (1.36) a.u., which reproduce the results of random-phase approximation (RPA) calculations.<sup>35</sup> The results of the d-COHSEX calculations for valence bandwidths and excitation energies are given in Table III, where comparison is made with

TABLE II. Self-consistent Hartree-Fock eigenvalues and gap  $E_g$  for diamond, as obtained in this work (LAPW) and in other calculations. LDA and experimental values are also given for comparison. Energies are measured in eV with respect to the valence-band maximum.

	LDA (eV)			HF (eV)			Expt. <sup>c</sup> (eV)
	PP <sup>a</sup>	LMTO <sup>b</sup>	LAPW	PP <sup>a</sup>	LMTO <sup>b</sup>	LAPW	
$\Gamma_{1v}$	-22.7	-21.3	-21.5	-29.1	-29.9	-29.4	-24.2
$\Gamma_{15c}$	5.5	5.7	5.6	15.0	14.6	14.7	7.3
$\Gamma_{2'c}$	12.3	13.4	13.4	24.8	23.7	24.5	15.3
$X_{1c}$	3.9		4.6	13.6	12.7	13.2	
$L_{1c}$			8.4		17.6	18.3	
$E_g$	3.4	4.1	4.0	12.9	12.1	12.4	5.5
$X_{4v} \rightarrow X_{1c}$	10.4		10.9	21.3	21.3	21.5	12.5
$L_{3'v} \rightarrow L_{1c}$	10.8		11.2	21.8	21.3	22.0	12.5

<sup>a</sup>Pseudopotential calculation, Ref. 18.

<sup>b</sup>LMTO calculation, Ref. 15

<sup>c</sup>From Ref. 29.

TABLE III. Valence-band width and excitation energies in silicon and diamond, as obtained in this work from a self-consistent d-COHSEX calculation, and compared to other calculations and experimental values. Energies are given in eV relative to the valence-band maximum.

	LDA	d-COHSEX	d-COHSEX <sup>a</sup>	d-COHSEX <sup>b</sup>	Expt.
Si					
$\Gamma_{1v}$	12.0	13.9			-12.5 <sup>c</sup>
$\Gamma_{15c}$	2.6	3.1	3.2		3.4 <sup>c</sup>
$\Gamma_{2'c}$	3.1	4.5	4.4		4.2 <sup>c</sup>
$X_{1c}$	0.6	0.4	0.8		1.3 <sup>d</sup>
$L_{1c}$	1.4	1.9	2.1		2.1 <sup>e</sup> 2.4 <sup>d</sup>
$E_g$	0.5	0.3	0.7	0.5	1.2 <sup>c</sup>
$X_{4v} \rightarrow X_{1c}$	3.5	3.8	4.2		4.2 <sup>d</sup> 4.5 <sup>c</sup>
$L_{3'v} \rightarrow L_{1c}$	2.6	3.3	3.5	3.3	3.5 <sup>c</sup> 3.9 <sup>d</sup>
C					
$\Gamma_{1v}$	21.5	25.1			24.2 <sup>c</sup>
$\Gamma_{15c}$	5.6	7.4			7.3 <sup>c</sup>
$\Gamma_{2'c}$	13.4	15.8			15.3 <sup>c</sup>
$X_{1c}$	4.6	5.2			
$L_{1c}$	8.4	10.3			
$E_g$	4.0	4.7		5.1	5.5 <sup>c</sup>
$X_{4v} \rightarrow X_{1c}$	10.9	12.5			12.5 <sup>c</sup>
$L_{3'v} \rightarrow L_{1c}$	11.2	13.5			12.5 <sup>c</sup>

<sup>a</sup>From Ref. 18.

<sup>b</sup>From Ref. 4.

<sup>c</sup>From Ref. 29.

<sup>d</sup>From Ref. 30.

<sup>e</sup>From Ref. 31.

the pseudopotential values of Refs. 18 and 4, which were obtained with the same model dielectric function. The agreement between these two calculations is very good, and a striking result is that the lowest direct excitation energies are now in satisfactory agreement with experimental data. However, as previously noticed (see, e.g., Ref. 18), the lowest indirect gaps are still considerably underestimated in this approximation.

#### IV. CONCLUSION

The major purpose of the present work was to show that the LAPW basis, which has been widely and successfully used in conventional LDA-based band structure calculations, is well suited also for HF-like computations. This was demonstrated by our self-consistent calculations for silicon and diamond, which are found to be in very good agreement with previous HF results. Our formalism retains the precision and efficiency of the corresponding LDA scheme, in particular regarding the evaluation of

potentials without shape approximation, the ease with which the convergence of the results with the basis-set size can be monitored, and finally the ability to treat all the elements of the Periodic Table.

Since HF is a well-defined starting point for perturbative many-body calculations, we have also derived the formalism for more sophisticated approaches like the GW and COHSEX approximations. The case of d-COHSEX, particularly simple to implement, has been applied to silicon and diamond, resulting in satisfactory values for the lowest direct excitation energies.

#### ACKNOWLEDGMENTS

It is a pleasure to acknowledge many stimulating discussions with F. Gygi. This work was supported by the Swiss National Science Foundation (Grant No. 30-272.90). The computations were performed in part at ETH-CSCS (Centro Svizzero di Calcolo Scientifico).

\* Present address: Dipartimento di Scienze Fisiche, Università Federico II di Napoli, Napoli, Italy.

<sup>†</sup> Also at Institut de Physique Appliquée, Ecole Polytechnique Fédérale, PHB Ecublens, CH-1015 Lausanne, Switzerland.

<sup>1</sup> *Theory of the Inhomogeneous Electron Gas*, edited by S. Lundqvist and N. H. March (Plenum, New York, 1983); R. O. Jones and O. Gunnarsson, *Rev. Mod. Phys.* **61**, 689 (1989), and references therein.

<sup>2</sup> G. Strinati, H. J. Mattausch, and W. Hanke, *Phys. Rev. B* **25**, 2867 (1982).

<sup>3</sup> S. Horsch, P. Horsch, and P. Fulde, *Phys. Rev. B* **29**, 1870 (1984).

<sup>4</sup> M. S. Hybertsen and S. G. Louie, *Phys. Rev. Lett.* **55**, 1418 (1985); *Phys. Rev. B* **32**, 7005 (1985).

<sup>5</sup> R. W. Godby, M. Schlüter, and L. J. Sham, *Phys. Rev. Lett.* **56**, 2415 (1986).

<sup>6</sup> R. D. Cowan, *Phys. Rev. B* **163**, 54 (1967); I. Lindgren, *Int.*

- J. Quantum Chem. **5**, 411 (1971); A. Zunger, J. P. Perdew, and G. L. Oliver, Solid State Commun. **34**, 933 (1980); J. P. Perdew and A. Zunger, Phys. Rev. B **23**, 5048 (1981).
- <sup>7</sup> A. Svane and O. Gunnarsson, Europhys. Lett **7**, 171 (1988); Phys. Rev. Lett. **65**, 1148 (1990); A. Svane, *ibid.* **68**, 1900 (1992).
- <sup>8</sup> R. G. Parr and W. Yang, *Density Functional Theory of Atoms and Molecules* (Oxford University Press, Oxford, 1989).
- <sup>9</sup> K. Laasonen, F. Csajka, and M. Parrinello, Chem. Phys. Lett. **194**, 172 (1992).
- <sup>10</sup> G. Ortiz and P. Ballone, Z. Phys. D **19**, 169 (1991).
- <sup>11</sup> V. I. Anisimov, J. Zaanen, and O. K. Andersen, Phys. Rev. B **44**, 943 (1991); V. I. Anisimov, M. A. Korotin, J. Zaanen, and O. K. Andersen, Phys. Rev. Lett. **68**, 345 (1992).
- <sup>12</sup> L. Hedin, Phys. Rev. **139**, A796 (1965).
- <sup>13</sup> C. Pisani and R. Dovesi, Int. J. Quantum Chem. **17**, 501 (1980); C. Pisani, R. Dovesi, and C. Roetti, *Hartree-Fock ab initio Treatment of Crystalline Systems*, Lecture Notes in Chemistry Vol. 68 (Springer-Verlag, Heidelberg, 1988).
- <sup>14</sup> J. M. André, Comput. Phys. Commun. **1**, 391 (1970); J. M. André, V. P. Bodart, J. L. Brédas, J. Delhalle, and J. G. Fripiat, in *Quantum Theory of Polymers: Solid State Aspects*, Vol. 123 of *NATO Advanced Study Institute, Series C: Mathematical and Physical Sciences*, edited by J. Ladik and J. M. André (Reidel, Boston, 1984).
- <sup>15</sup> A. Svane, Phys. Rev. B **35**, 5496 (1987).
- <sup>16</sup> A. Svane and O. K. Andersen, Phys. Rev. B **34**, 5512 (1986).
- <sup>17</sup> I. Ohkoshi, J. Phys. C **18**, 5415 (1985).
- <sup>18</sup> F. Gygi and A. Baldereschi, Phys. Rev. B **34**, 4405 (1986).
- <sup>19</sup> F. Gygi, Ph.D. thesis, Ecole Polytechnique Fédérale, Lausanne, 1988.
- <sup>20</sup> D. D. Koelling and G. O. Arbman, J. Phys. F **5**, 2041 (1975); O. K. Andersen, Phys. Rev. B **12**, 3060 (1975).
- <sup>21</sup> H. J. F. Jansen and A. J. Freeman, Phys. Rev. B **30**, 561 (1984), and references therein.
- <sup>22</sup> S. Massidda, M. Posternak, and A. Baldereschi, Phys. Rev. B **46**, 11 705 (1992).
- <sup>23</sup> For clarity reasons we will describe, here and in the following, the spin-restricted case (no spin indices will be used). The spin-unrestricted generalization is straightforward. In the case of spin-unrestricted systems, the similarity of HF and LSD wave functions is not always existent.
- <sup>24</sup> M. Weinert, J. Math. Phys. **22**, 2433 (1981).
- <sup>25</sup> L. Dagens and F. Perrot, Phys. Rev. B **5**, 641(1972); **8**, 1281 (1973).
- <sup>26</sup> F. Perrot, Phys. Status Solidi B **52**, 163 (1972).
- <sup>27</sup> Obviously, in a plane-wave pseudopotential formalism, there is no need to distinguish between  $\bar{\rho}$ ,  $\rho$ , and  $\rho$ .
- <sup>28</sup> F. Gygi (unpublished).
- <sup>29</sup> *Zahlenwerte und Funktionen aus Naturwissenschaften und Technik*, edited by O. Madelung, Landolt-Börnstein, New Series, Group III, Vol. 17a (Springer, New York, 1982).
- <sup>30</sup> D. Straub, L. Ley, and F. J. Himpsel, Phys. Rev. Lett. **54**, 142 (1985).
- <sup>31</sup> R. Hulthen and N. G. Nilsson, Solid State Commun. **18**, 1341 (1976).
- <sup>32</sup> D. J. Chadi and M. L. Cohen, Phys. Rev. B **8**, 5747 (1973).
- <sup>33</sup> W. von der Linden, P. Fulde, and K. P. Bohnen, Phys. Rev. B **34**, 1063 (1986).
- <sup>34</sup> R. Dovesi, M. Causà, and G. Angonoa, Phys. Rev. B **24**, 4177 (1981).
- <sup>35</sup> A. Baldereschi and E. Tosatti, Phys. Rev. B **17**, 4710 (1978).